Available online at www.sciencedirect.com
ScienceDirect
Journal of Power Sources 170 (2007) 412–418
JOURNAL OF POWER SOURCES
www.elsevier.com/locate/jpowsour

Hydrogen generation system using sodium borohydride for operation of a 400 W-scale polymer electrolyte fuel cell stack

Sun Ja Kim [a,b], Jaeyoung Lee [a,*], Kyung Yong Kong [a], Chang Ryul Jung [a], In-Gyu Min [a], Sang-Yeop Lee [a], Hyoung-Juhn Kim [a], Suk Woo Nam [a,**], Tae-Hoon Lim [a]

[a] *Center for Fuel Cell Research, Korea Institute of Science and Technology, Seoul 136-791, Republic of Korea*
[b] *School of Engineering, University of Science and Technology, Daejeon 305-333, Republic of Korea*

Received 15 January 2007; accepted 28 March 2007
Available online 22 April 2007

Abstract

Sodium borohydride ($NaBH_4$) in the presence of sodium hydroxide as a stabilizer is a hydrogen generation source with high hydrogen storage efficiency and stability. It generates hydrogen by self-hydrolysis in aqueous solution. In this work, a Co–B catalyst is prepared on a porous nickel foam support and a system is assembled that can uniformly supply hydrogen at >6.5 L min^{-1} for 120 min for driving 400-W polymer electrolyte membrane fuel cells (PEMFCs). For optimization of the system, several experimental conditions were changed and their effect investigated. If the concentration of $NaBH_4$ in aqueous solution is increased, the hydrogen generation rate increases, but a high concentration of $NaBH_4$ causes the hydrogen generation rate to decrease because of increased solution viscosity. The hydrogen generation rate is also enhanced when the flow rate of the solution is increased. An integrated system is used to supply hydrogen to a PEMFCs stack, and about 465 W power is produced at a constant loading of 30 A.

Keywords: Sodium borohydride; Hydrogen generation; Co–B catalyst; Polymer electrolyte fuel cell

1. Introduction

In response to the ever-increasing demands for power in portable electronic devices as more enhanced features and complexity are introduced to them, fuel cells have attracted much attention as replacements for lithium batteries. Among the various types of fuel cell, direct liquid fuel cells (DLFCs) have emerged as strong candidates due, in large part, to the advantages of using a liquid fuel. Even though hydrogen-powered polymer electrolyte membrane fuel cells (PEMFCs) operate more efficiently with higher power densities than DLFCs, hydrogen supply has been an obstacle to the application of PEMFCs in portable power sources.

Hydrogen has been stored in tanks in compressed or liquefied form, in hydrogen-storing alloys, and on activated carbon or nanoscale materials such as carbon nanotubes. None of these methods are suitable for portable applications due to the low volumetric and gravimetric efficiency of hydrogen storage as well as the associated safety issues [1–5]. Instead of such hydrogen storage methods, liquid fuels (methanol, ethanol, gasoline, etc.) and chemical hydrides ($NaBH_4$, KBH_4, LiH, NaH, etc.) could be employed as hydrogen sources for portable PEMFC. In the case of liquid fuels, however, high-temperature reforming processes are too complex to satisfy the requirements of portable PEMFC operation. Among the chemical hydrides, sodium borohydride ($NaBH_4$) has been intensively studied as a hydrogen storage material because of its advantages of nonflammability and stability in air, easily controlled hydrogen generation rate, side product recycleability, and high hydrogen storage efficiency. Previous studies on hydrogen production from $NaBH_4$ have been summarized in a recent review [6]. Base-stabilized $NaBH_4$ solution hydrolyzes to hydrogen and sodium metaborate ($NaBO_2$) only when in contact with specific catalysts. The

* Corresponding author. Present address: Department of Environmental Science and Engineering, GIST, Gwangju 500-712, Republic of Korea.
Tel.: +82 62 970 2440; fax: +82 62 970 2434.
** Corresponding author.
E-mail addresses: jaeyoung@gist.ac.kr (J. Lee), swn@kist.ac.kr (S.W. Nam).

0378-7753/$ – see front matter © 2007 Elsevier B.V. All rights reserved.
doi:10.1016/j.jpowsour.2007.03.083

reaction equation is as follows:

$$NaBH_4 + 2H_2O \rightarrow NaBO_2 \cdot xH_2O + 4H_2 + \text{heat} \quad (x = 2 \text{ or } 4) \tag{1}$$

It is possible to generate more hydrogen using $NaBH_4$ solution in the presence of a catalyst. It is reported that some metals are useful catalysts [7–10], but most of them are precious metals that are expensive. According to our previous study [8], the Co–B catalyst (see below) is easy to make, is competitive with the above-mentioned metals, and possesses a high hydrogen-generation ability.

In the research presented here, a hydrogen generation system using $NaBH_4$ is developed for the operation of 400-W PEMFCs. This system could be applied to robots for dealing with hazardous conditions, emergency power supply equipment, and military and portable transportation (e.g., scooters [11]).

2. Experimental and system design

2.1. Catalyst preparation

Following a previous study [8], 40 wt.% cobalt chloride ($CoCl_2$, DAEJUNG) solution and 20 wt.% $NaBH_4$ (DAEJUNG) solution with 1 wt.% NaOH were used for the preparation of the Co–B catalyst on Ni foam by a simple dipping procedure. The Ni foam used in this study was 20 mm (l) × 30 mm (w) × 1.4 mm (t) and weighed 250 ± 20 mg. The Ni foam was dipped into $CoCl_2$ solution for 10 s and then into $NaBH_4$ solution for 10 s. These successive two steps were repeated five times and the resulting Ni foam was washed with distilled water. Preparation of the Co–B/Ni foam catalyst was completed after 15 dipping steps. For stable generation of hydrogen with fast initiation, the Co–B catalyst was calcined at 250 °C for 2 h under a hydrogen and argon atmosphere in accordance with previous research [8].

Two different reactors were constructed as follows. Pieces of Co–B catalyst were fixed in stainless-steel (SUS) cases A and B of different size, (see Fig. 1(a) and (b)), respectively. Three pieces of Co–B catalyst were fixed in the A reactor (90 mm × 40 mm × 15 mm). The inlet was 1/8 in. SUS tube and the outlet 1/4 in. SUS tube. For increased hydrogen generation, the B reactor was sized correspondingly (100 mm × 65 mm × 15 mm). Nine pieces of Co–B catalysts were place in this reactor, see Fig. 1(d). The inlet size was the same as that of the A reactor and the outlet size was increased to 3/8 in. SUS tube to avoid inhomogeneous pressure distribution inside the second reactor. The reactors were wrapped with Kaowool® (1 mm thickness, Thermal Ceramics) to maintain the reaction temperature roughly constant, i.e., for consistent

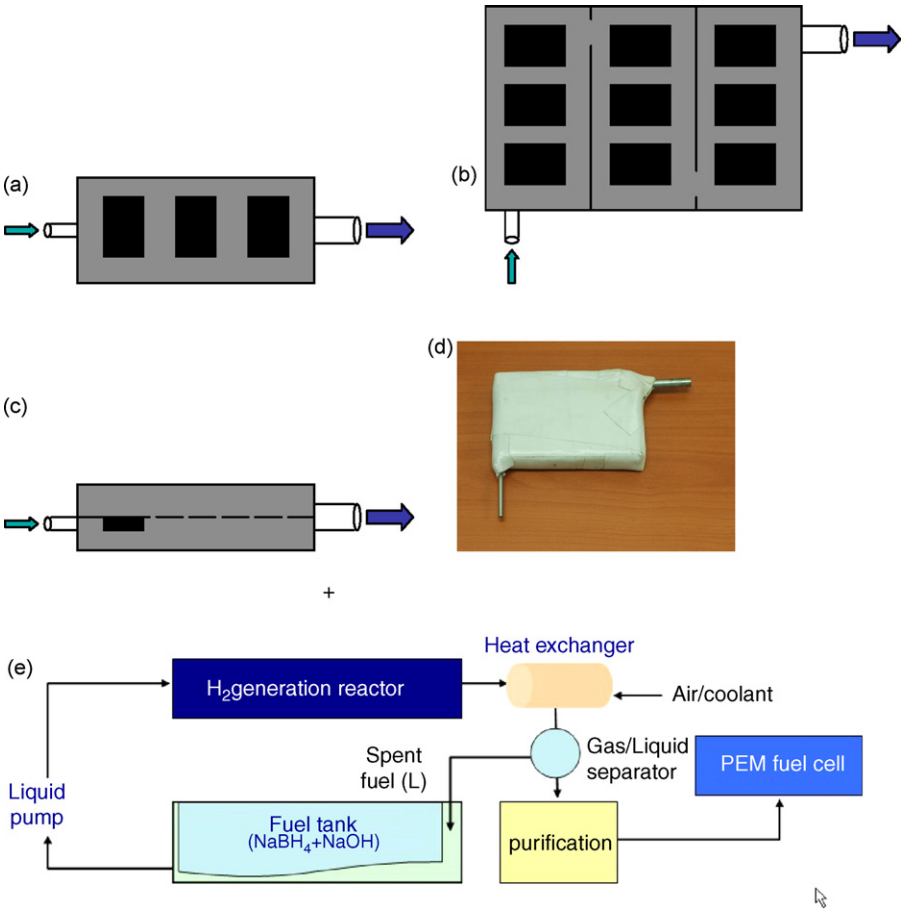

Fig. 1. (a) Reactor design of reactor A (three-catalysts). (b) Reactor design of reactor B (nine-catalysts). (c) Schematic of fuel feeding and hydrogen generation in the reactor B. (d) Photograph of a reactor B. (e) Simplified experimental procedure for hydrogen generation.

reaction rate without fluctuation. The generation of hydrogen from $NaBH_4$ is strongly dependent on reaction temperature.

2.2. Hydrogen generation

There are several factors that influence the rate of hydrogen generation. Experiments were carried out to investigate the effect of the following parameters: (i) $NaBH_4$ concentration; (ii) NaOH concentration; (iii) flow rate of $NaBH_4$ solution. The $NaBH_4$ concentration was varied as follows: 10, 15, 20, 25 and 30 wt.% with 1 wt.% NaOH solution at a flow rate of 15 mL min^{-1}. The NaOH concentration was varied as follows: 0, 0.5, 1.0, 2.0 and 4.0 wt.% in the presence of 20 wt.% $NaBH_4$ and a 15 mL min^{-1} flow rate of the solution. The flow rate of the solution was controlled by a Master Flex pump and varied at 10, 12.5, 15, 17.5, and 20 mL min^{-1} with 20 wt.% $NaBH_4$ and 1 wt.% NaOH. Each experiment was executed for 20 min. The hydrogen generation rate and reaction temperature were measured with a mass flow meter (MFM, F-111C, Bronkhorst) and a temperature recorder (NI 9211, National Instruments), respectively. A simplified diagram of hydrogen generation and separation is shown in Fig. 1(e).

2.3. Integrated system of hydrogen generation

Based on experimental observations in the above hydrogen generation experiments, home-made components with lining were integrated inside a SUS case. The hydrogen generation system developed was composed of a fuel tank, fuel feeding pump, hydrogen generation reactor, gas–liquid separator 1, heat-exchanger, gas–liquid separator 2, and an absorption tank. The fuel tank was a flexible base-resistant bag (polypropylene) for continuous feeding of liquid fuels. The hydrogen generation reactor contained nine pieces of catalyst, and they were evenly separated in a reactor. Gas–liquid separator 1 was a copper hexahedral box. Copper pipe of 4-mm outer diameter was rolled inside the gas–liquid separator 1. The heat-exchanger was made of copper pipe of 1/4 in. diameter and was curved to increase the heat-transfer area. Gas–liquid separator 2 was a stainless-steel L-shaped box fitted with a fan. A brass cylinder acted as an absorption tank for absorption of any eventual liquid impurities. Two small bags that each contained 2 g of super absorbent materials (SAM, polyacrylate containing sodium salt, KOLON CHEMICAL) are placed in the cylinder. The cooling section was composed of a coolant tank, a coolant pump (NF5, KNF), a radiator, and the inner copper pipe of gas–liquid separator 1. Coolant composed of a mixture of water and ethanol with a volume ratio of 7:3 circulated through the cooling lines. The radiator was made of copper cooling fins mounted on an aluminum box with a cooling fan placed on it. A 1/8 in. SUS tube placed inside gas–liquid separator 2 was connected to the liquid pump for returning spent fuel into the compressed flexible base-resistant bag (polypropylene).

The power-conditioning control board was designed for controlling the apparatus, namely, a on-off switch, a rechargeable lithium-ion battery (11.1 V, 3000 mA), a fuel feeding pump, a coolant pump, a return pump, and a number of fans. A battery of about 30 Wh was used for initial start-up. Cooling fans of different power capacity and dimensions were located throughout the whole system except for the fuel tank area. The total power consumption of the system was 20.74 Wh for 2 h of operation. The whole integrated system was 520 mm × 240 mm × 100 mm in size and weighed 11.41 kg.

The temperature distribution in the total system was measured with a thermal imager (IRI 1001E, InfraRed Integrated Systems). Images were taken at intervals of 30 min from system start-up.

2.4. Connecting to PEMFC single cell and stack

In order to apply the hydrogen generation system to operate high capacity devices, the system was connected to a PEMFC single cell, and stack. Single-cell testing was performed at a low hydrogen generation rate as controlled by the $NaBH_4$ flow rate. After that, a stack test was performed at a normal hydrogen generation rate. Single cell conditioning was uundertaken according to Prasanna's work [12].

A single cell having 25 cm^2 of active electrode area was prepared. Hydrogen was fed to the anode at a flow rate of 0.4 L min^{-1}. Air was fed to the cathode at a flow rate of 1.2 L min^{-1}. Both gases passed a humidifier before entering a single cell. Current–voltage (*I–V*) characteristics were measured from 0 to 2000 mA cm^{-2} at a cell temperature of 80 °C. The current loading was operated by a dc, electronic load (EL-1000P, DAE GIL ELECTRONICS). The PEMFC stack was made by joining 22 single cells, each single cell had area of 71 cm^2. Hydrogen was fed to the anode at a flow rate of 6.5 L min^{-1}, while air was fed to the cathode at 24 L min^{-1}. Gases were fed to the stack without passing through the operating humidifier. The cell temperature was 40 °C. Tests were made of power generation at a constant current of 30 A operated by an electronic load (FCTS-1kW-200A-32V-20/50 slpm, ARBIN INSTRUMENTS).

3. Results and discussion

3.1. Hydrogen generation

When the smaller reactor (three small catalysts) is used, a supply of 20.3 mL min^{-1} of $NaBH_4$ solution generates 3.05 L min^{-1} of hydrogen (see Fig. 2). On the other hand, when the reactor consisting of nine catalysts is used, 20 mL min^{-1} of $NaBH_4$ solution generated 6.27 L min^{-1} of hydrogen (see Fig. 5). Thus, the higher the amount of catalyst, the more hydrogen is generated. Fig. 1(c) shows that the catalyst is interfaced between the liquid and the gas in the reactor. As seen in Fig. 1(b), the reactor is designed for homogeneous hydrolysis.

The pattern of the hydrogen generation rate following the concentration of $NaBH_4$ of the solution is shown in Fig. 3. The hydrogen generation rates of 10, 15, 20, 25 and 30 wt.% $NaBH_4$ solutions were 3.23, 4.55, 5.36, 5.47 and 4.69 L min^{-1}, respec-

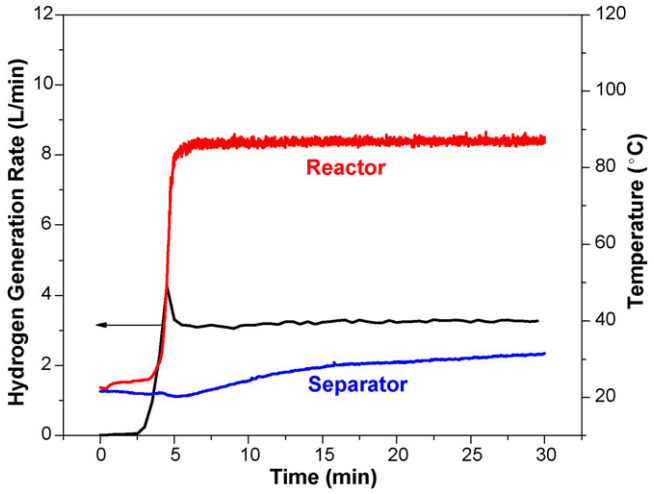

Fig. 2. Hydrogen generation rate and temperature of hydrogen generator reactor and gas–liquid separator using reactor A. $NaBH_4$ = 20 wt.%, NaOH = 1 wt.%, flow rate = 20.3 mL min^{-1}.

tively. When the $NaBH_4$ concentration in aqueous solution is increased, the hydrogen generation rate was also increased. As in our study, Kojima et al. [9] observed an increasing hydrogen generation rate in range of 8.6–25 wt.% $NaBH_4$. Too high a concentration of $NaBH_4$ lowered the hydrogen generation. According to reaction (1), sodium metaborate ($NaBO_2$) exists as a hydrate in the solution. When the $NaBH_4$ concentration is increased, the produced $NaBO_2$ consumes more and more water. It leads to higher solution viscosity which hinders contact of the $NaBH_4$ solution with the catalyst. As a result, the hydrogen generation rate appears to decrease. Amendola et al. [10] also observed a similar influence on the hydrogen generation rate when using a higher concentration of $NaBH_4$. The optimal concentration of $NaBH_4$ for maximum hydrogen generation was 12.5 wt.%, which is slightly lower than the concentration observed in our study. We assume that the different catalyst used in Amendola's work explains the difference in results.

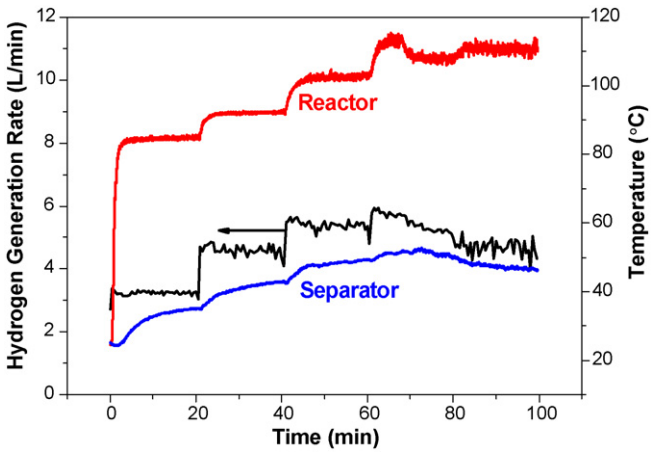

Fig. 3. Hydrogen generation rate and temperature of solution. $NaBH_4$ concentration: (a) 10, (b) 15, (c) 20, (d) 25 and (e) 30 wt.%. NaOH = 1 wt.%. Flow rate = 15 mL min^{-1}.

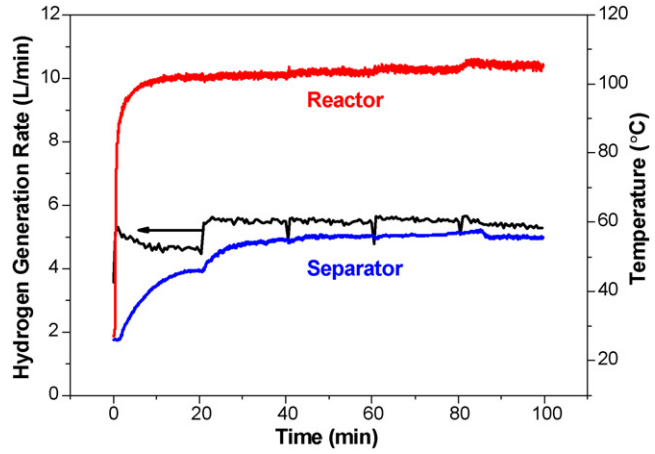

Fig. 4. Hydrogen generation rate and temperature of solution. NaOH concentrations: (a) 0, (b) 0.5, (c) 1.0, (d) 2.0 and (e) 4.0 wt.%. $NaBH_4$ = 20 wt.%, Flow rate = 15 mL min^{-1}.

Self-hydrolysis of $NaBH_4$ occurs in water and this affects the rate of hydrogen generation. To increase solution stability, i.e., to inhibit self-hydrolysis, the pH of the solution was increased by adding alkali (NaOH). The influence of pH on the half-life of $NaBH_4$ decomposition is as follows [10]:

$$\log t_{1/2} = \text{pH} - (0.034T - 1.92) \quad (2)$$

where $t_{1/2}$ is the half-life of $NaBH_4$ decomposition (min) and T is the solution temperature (K). At pH 12 and 298 K, the solution remains stable for 4 days. The change in the rate of hydrogen generation with addition of NaOH to the solution is presented in Fig. 4. The hydrogen generation rates from $NaBH_4$ solution with 0, 0.5, 1.0, 2.0 and 4.0 wt.% NaOH are 4.75, 5.46, 5.48, 5.53 and 5.39 L min^{-1}, respectively. Thus, it is clear that the addition of NaOH does not change the hydrogen generation rate except at 0 wt.% of NaOH. In case of the solution without NaOH, hydrogen bubbles produced by self-hydrolysis disturb the flow to the reactor and there by induce an irregular supply of $NaBH_4$ solution. Therefore, the hydrogen generation rate is expected to become lower. By contrast, Kojima et al. [9] found

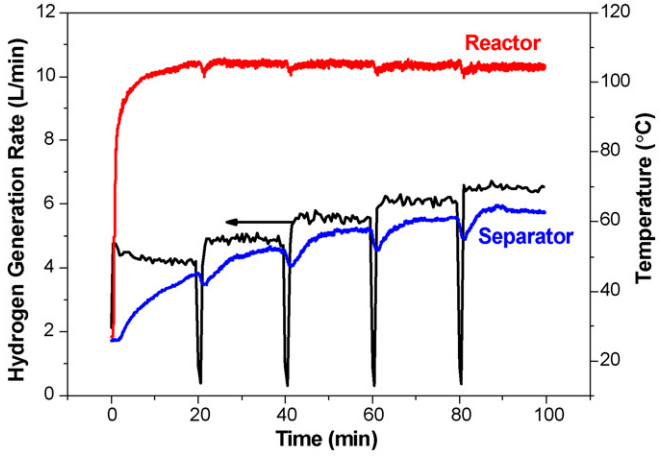

Fig. 5. Hydrogen generation rate and feed solution temperature. Flow rates: (a) 10, (b) 12.5, (c) 15, (d) 17.5 and (e) 20 mL min^{-1}. $NaBH_4$ = 20 wt.%, NaOH = 1 wt.%.

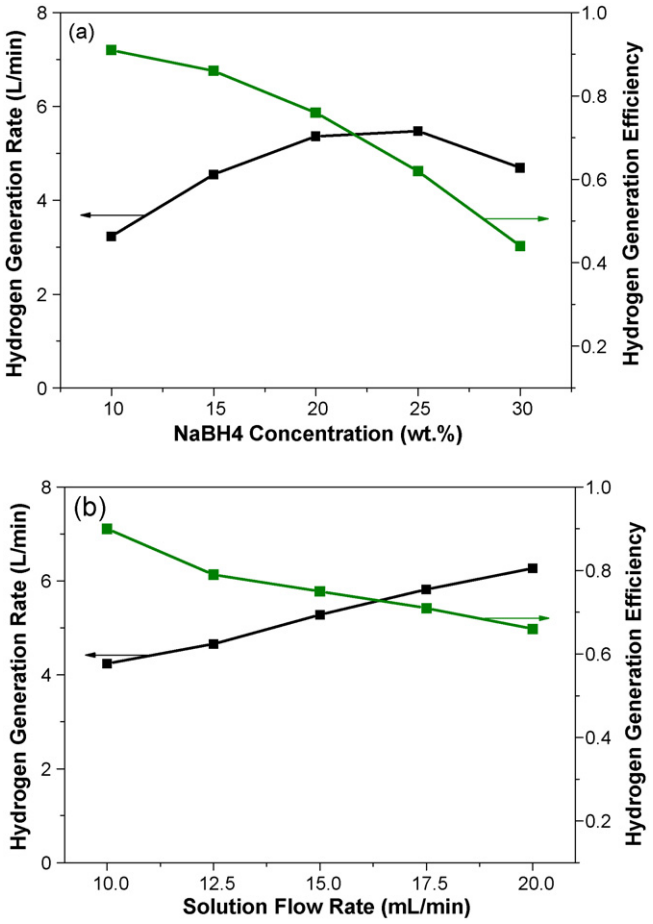

Fig. 6. (a) Hydrogen generation rate and efficiency with $NaBH_4$ concentration. (b) Hydrogen generation rate and efficiency with solution flow rate.

no difference in the hydrogen generation rate between 0 and 4 wt.% NaOH. We conclude that this is due to their use of a higher flow rate (200 mL min^{-1}) and consequent by a consistent supply of solution independent of the pressure drop inside the reactor compared with our study (15 mL min^{-1}).

The variation of hydrogen generation rate with the flow rate of the solution is given in Fig. 5. The hydrogen generation rates at 10, 12.5, 15, 17.5 and 20 mL min^{-1} of $NaBH_4$ solution are 4.24, 4.66, 5.28, 5.82 and 6.27 L min^{-1}, respectively. These data show that a faster flow rate gives rise to an increased rate of hydrogen generation. It is concluded that the hydrogen generation rate is strongly dependant on the $NaBH_4$ solution flow rate under certain conditions (e.g., temperature > 100 °C).

The hydrogen generation efficiency η is calculated via the following equation:

$$\eta = \frac{\text{real } H_2 \text{ generation}}{\text{theoretical } H_2 \text{ generation}} = \frac{V}{u \times x/38 \times 4 \times 22.4} \quad (3)$$

where V is the hydrogen generation rate (L min^{-1}), u the solution flow rate (mL $min^{-1} \approx$ g min^{-1}) and x is the $NaBH_4$ concentration. In Eq. (3) the values 38, 4 and 22.4 represent the $NaBH_4$ molecular weight, moles of hydrogen generation per a mole of $NaBH_4$ and gas volume per mole, respectively.

Fig. 6(a) shows the hydrogen generation rate and efficiency as a function of the $NaBH_4$ concentration. The hydrogen generation efficiencies of $NaBH_4$ solutions of 10, 15, 20, 25 and 30 wt.% are 0.91, 0.86, 0.76, 0.62 and 0.44, respectively. Considering both the hydrogen rate and efficiency, we selected the 20 wt.% $NaBH_4$ solution as the optimum value. Fig. 6(b) shows the hydrogen generation rate and efficiency following the flow rate. Hydrogen generation efficiencies for flow rates of 10, 12.5, 15, 17.5 and 20 mL min^{-1} $NaBH_4$ solution are 0.9, 0.79, 0.75, 0.71, and 0.66, respectively. Considering both hydrogen generation rate and efficiency, 15 mL min^{-1} is chosen as the solution flow rate. 1 wt.% NaOH was added to the solution in our system.

3.2. Integrated system of hydrogen generation

Based on the results of the above experiments, a hydrogen generation system was designed and built in our laboratories. As mentioned earlier, the system consists of five main processes: (a) fuel feeding; (b) hydrogen generation; (c) separation of gas–liquid product; (d) return of spent fuel; (e) purification of hydrogen. A schematic of the system and process flow diagram is shown in Fig. 7(a) and (b), respectively.

Following the results of the initial hydrogen generation experiments (Figs. 3–5), the optimum concentration and flow rate were determined. The size of fuel tank is 2.1 L and it contains 20 wt.% $NaBH_4$ with 1 wt.% NaOH aqueous solution. $NaBH_4$ solution is supplied by a liquid pump (NF5, KNF) from the fuel tank and it is passed through the reactor, at which point hydrogen is generated. The fuel feeding pump is operated at a maximum of 6 V dc. The fuel flow rate is controlled at 2.1 V by a power-conditioning control board appropriate to the target hydrogen generation rate. The power consumption of the fuel feeding pump is 0.54 W. Hydrogen gas and by-product are separated via two consecutive gas–liquid separators and a liquid absorption tank.

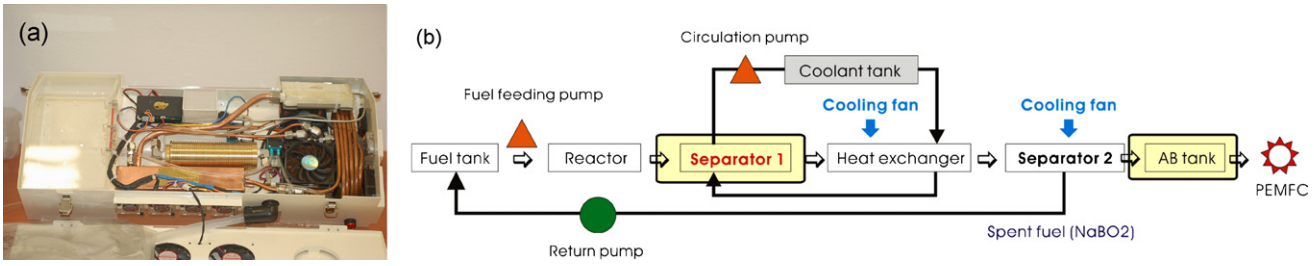

Fig. 7. (a) Photograph of integrated system. (b) Process flow diagram of system.

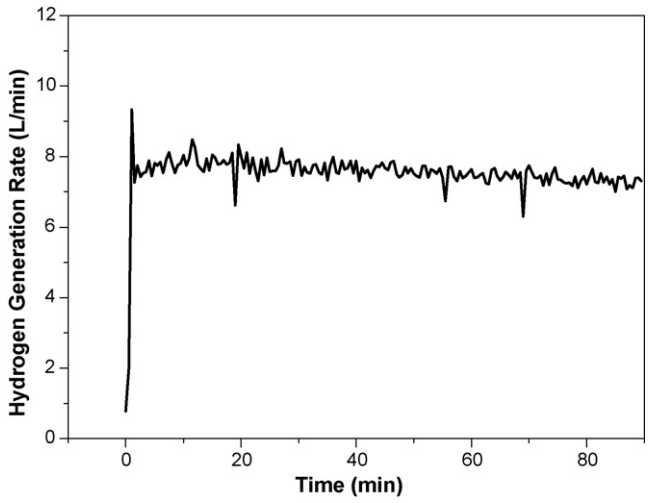

Fig. 8. Hydrogen generation rate of system. $NaBH_4$ = 20 wt.%, NaOH = 1 wt.%, flow rate = 18.4 mL min^{-1}.

Gas–liquid separator 1 is installed for cooling the products. Gaseous product leaving the reactor is composed not only of hydrogen but also of water and by-product vapour. If water vapour containing sodium hydroxide is supplied to PEMFCs, the stack may become damaged, and for this reason hydrogen and by-product separation is vital. Products must not necessarily be cooled to low temperature to separate gas from mixed product. The product forms over a curved copper pipe, cooled by fans, which acts as a heat-exchanger. Gas–liquid separator 2 is set up for separation of pure hydrogen and liquid by-product ($NaBO_2 \cdot xH_2O$). In general, about 75–80% spent fuel compared with fresh fuel is produced, i.e., 2.1 L of $NaBH_4$ solution generated about 1.7 L of by-product. This is much higher than the volume of gas–liquid separator 2, and thus, a recycling process is needed. By-product is returned to the spent fuel tank periodically by a pump (NF10KPDC, KNF). This step is also accompanied by a decrease in the product temperature, so that separation can be continued for a long period. The ratio, off-time/on-time of the return pump is about 10:1. The flow rate of the return pump is 150 mL min^{-1}. The power consumption of the coolant pump is 3.6 W.

An absorption tank with SAM bags was selected for purifying the hydrogen gas. Super absorbent materials (SAM) can absorb liquids at about 120 times of their own weight. A radiator, fitted with a fan and large-area fins, is installed to cool the coolant liquid warmed in the process. The coolant pump flow rate is 66 mL min^{-1}. Power consumption is 0.84 W.

The hydrogen generation rate of the system is shown in Fig. 8. The system produce about 7.5 L min^{-1} with small fluctuations

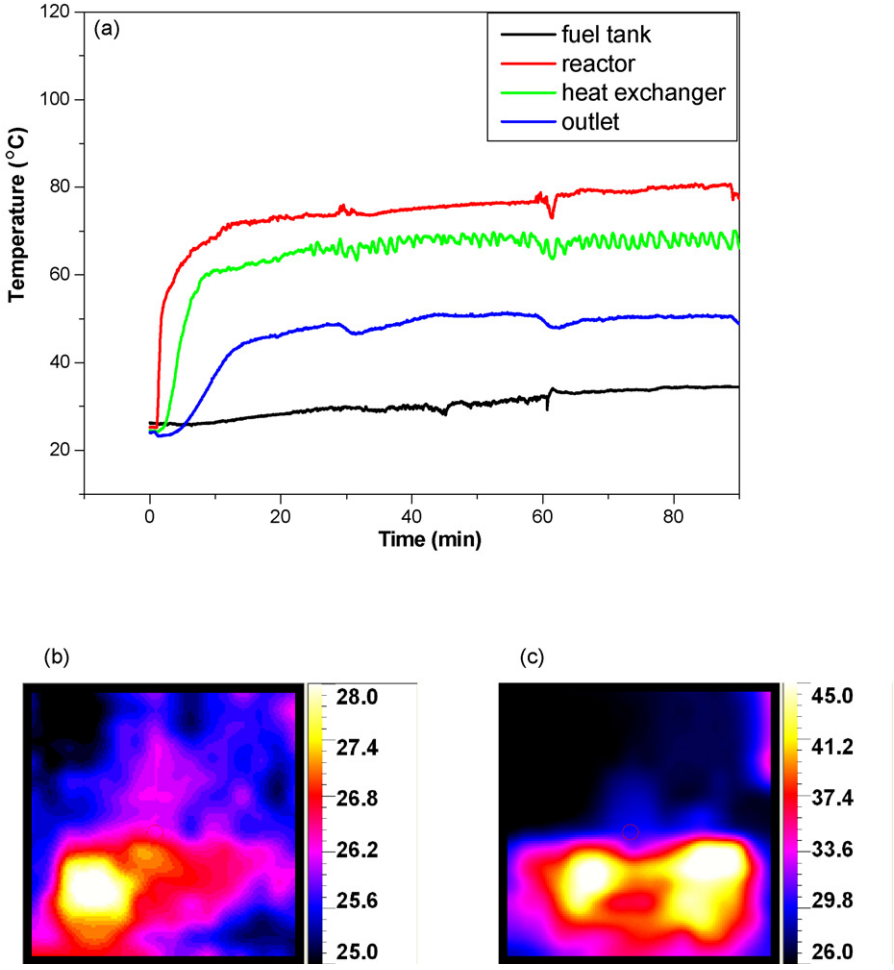

Fig. 9. (a) Temperature of system. (b and c) Thermal images of system at 0 and 60 min, respectively.

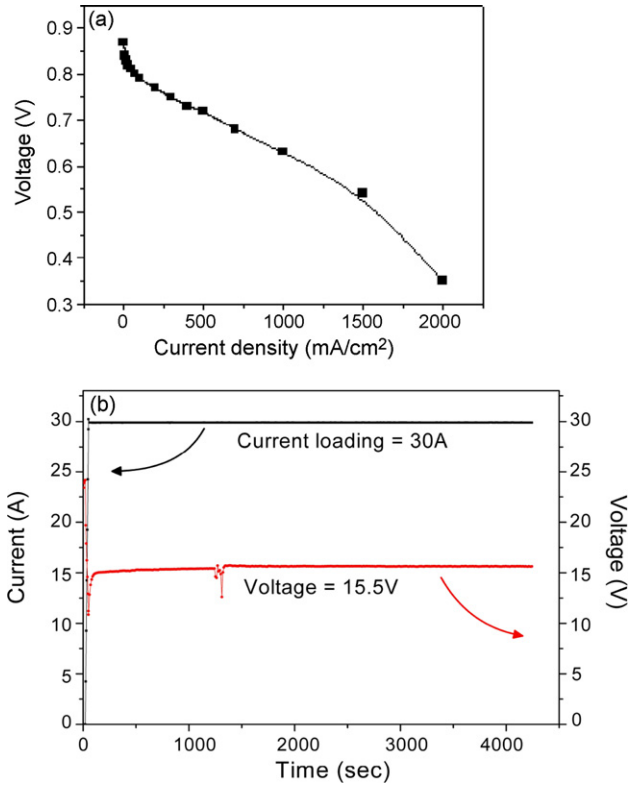

Fig. 10. (a) Single cell *I–V* curve at 80 °C. (b) Power generation of PEMFC stack at 30 A.

over 90 min of oepration. The flow rate is 18.4 mL min^{-1}. This is higher compared with previous hydrogen generation experiments due to the lower pressure drop with the optimized system components, e.g., the widened flow channel. The hydrogen generation efficiency is 0.87. About 55 mL liquid after passing the absorption tank has a pH of 8.39. Compared with the initial pH of the fuel (12.472), this shows that the NaOH is almost completely removed during passage through the system.

The data presented in Fig. 9(a) show that the temperature distribution of four different system areas is maintained fairly constant, which indicates that the different zones have no influence on temperature change. The system is well separated and isolated. The temperature of the liquid fuel is initially ~25 °C and reaches ~105 °C during heating by the exothermal reaction. It drops to 60 °C after the highly efficient heat-exchanger and further to 40 °C at the outlet of the hydrogen after the purification process. Typical thermal IR images of a system at 0 and 60 min are shown in Fig. 9(b) and (c) and clearly distinguish the temperature distribution of the system. Interestingly, through wrapping with a thermal insulator, the reactor area does not run at such a high temperature as the gas–liquid separator region. As shown in the images, the purification and outlet show relatively lower temperatures; this is in good agreement with the data in Fig. 9(a).

3.3. Connection to single cells and a stack

The product hydrogen was supplied to single PEMFC cell and stack. The flow rate of $NaBH_4$ fuel was 17.5 mL min^{-1} and the hydrogen generation rate was >6.0 L min^{-1}. The current–voltage curve of a single cell is given in Fig. 10a. The open-circuit voltage is 0.87 V and the cell voltage is 0.63 V at 1.0 A cm^{-2}. This indicates that the hydrogen extracted from $NaBH_4$ does not contain impurities (e.g. NaOH). The power performance of the PEMFC stack is shown in Fig. 10(b); 465 W is produced at 30 A for 70 min.

4. Conclusions

Based on various experimental observations, a hydrogen generation system using Co–B/Ni foam from $NaBH_4$ solution has been developed. The system can produce >6 L min^{-1} of hydrogen. This is sufficient to operate a 450-W PEMFC stack. The operating conditions required to do this are: optimism flow rate of $NaBH_4$ aqueous solution = 17.5 mL min^{-1}; appropriate concentrations of $NaBH_4$ and NaOH in the feed solution = 20 and 1 wt.%, respectively. The system consists of five parts: hydrogen generation, spent fuel retrieval, product cooling, gas-liquid separation, and purification. In addition, a power-conditioning control board is installed to provide system control. Connecting the system to PEMFC stacks gives no deleterious reactions. The system appears to offer promising applications in various industrial fields.

Acknowledgements

This research was supported by the Hydrogen Energy R&D Center, one of the 21st Century Frontier R&D Program, funded by the Ministry of Science and Technology of Korea.

References

[1] A. Ciancia, G. Pede, M. Brighigna, V. Perrone, Int. J. Hydrogen Energy 21 (1996) 397.
[2] K. Pehr, P. Sauemann, O. Traeger, M. Bracha, Int. J. Hydrogen Energy 26 (2001) 777.
[3] H.S. Roh, K.W. Jun, W.S. Dong, J.S. Chang, S.E. Park, Y.I. Joe, J. Mol. Catal. A 181 (2002) 137.
[4] D.L. Stojic, M.P. Marceta, S.P. Sovilj, S.S. Miljanic, J. Power Sources 118 (2003) 315.
[5] H.I. Schlesinger, H.C. Brown, A.E. Finholt, J.R. Gilbreath, H.R. Hoekstra, E.K. Hyde, J. Am. Chem. Soc. 75 (1953) 215.
[6] Y. Kojima, T. Haga, Int. J. Hydrogen Energy 28 (2003) 989.
[7] H.C. Brown, C.A. Brown, J. Am. Chem. Soc. 84 (1962) 1493.
[8] J. Lee, K.Y. Kong, C.R. Jung, T.G. Lee, E.A. Cho, S. Yoon, J. Han, S.W. Nam, Catal. Today 120 (2007) 305.
[9] Y. Kojima, K. Suzuki, K. Fukumoto, Y. Kawai, M. Kimbara, H. Nakanishi, S. Matsumoto, J. Power Sources 125 (2004) 22.
[10] S.C. Amendola, S.L. Sharp-Goldman, M.S. Janjua, N.C. Spencer, M.T. Kelly, P.J. Petillo, M. Binder, Int. J. Hydrogen Energy 25 (2000) 969.
[11] "Successful testing of fuel cell scooter in Korea", Fuel Cells Bull. 1 (2005) 11.
[12] M. Prasanna, E.A. Cho, H.-J. Kim, T.-H. Lim, I.-H. Oh, S.-A. Hong, J Power Sources 160 (2006) 90.